Appl. Math. Mech. -Engl. Ed., **37**(8), 987–998 (2016)
DOI 10.1007/s10483-016-2112-8

Applied Mathematics and Mechanics (English Edition)

Effect of particles on turbulent thermal field of channel flow with different Prandtl numbers*

Caixi LIU[1], Yuhong DONG[1,2,†]

1. Shanghai Institute of Applied Mathematics and Mechanics, Shanghai University, Shanghai 200072, China;
2. Shanghai Key Laboratory of Mechanics in Energy Engineering, Shanghai University, Shanghai 200072, China

Abstract The direct numerical simulation (DNS) of heat transfer in a fully developed non-isothermal particle-laden turbulent channel flow is performed. The focus of this paper is on the modulation of the particles on turbulent thermal statistics in the particle-laden flow with three Prandtl numbers ($Pr = 0.71$, 1.5, and 3.0) and a shear Reynolds number ($Re_\tau = 180$). Some typical thermal statistics, including normalized mean temperature and their fluctuations, turbulent heat fluxes, Nusselt number and so on, are analyzed. The results show that the particles have less effects on turbulent thermal fields with the increase of Prandtl number. Two reasons can explain this. First, the correlation between fluid thermal field and velocity field decreases as the Prandtl number increases, and the modulation of turbulent velocity field induced by the particles has less influence on the turbulent thermal field. Second, the heat exchange between turbulence and particles decreases for the particle-laden flow with the larger Prandtl number, and the thermal feedback of the particles to turbulence becomes weak.

Key words direct numerical simulation (DNS), Prandtl number, particle, thermal statistic, channel flow

Chinese Library Classification O359
2010 Mathematics Subject Classification 76T20

1 Introduction

The problems of heat transfer in the turbulent flow with laden particles are very important in nature and engineering[1–4], for instance, coal combustion, gas turbine, heat exchangers, and nuclear reactors. For the particle-laden turbulent flow, due to the dispersion of the particles in the turbulence, the particles as medium have the contribution of momentum and thermal transport to the turbulence. Therefore, the heat transfer of particle-laden flow is controlled by both turbulence and particles. It is known that many attempts have mainly focused on the study of heat transfer of particle-free turbulent flow. However, the study of turbulent heat transfer in the particle-laden turbulent flow is relatively little due to the complexity of the interaction between turbulence and particles. Therefore, the study of heat transfer in the

* Received Dec. 25, 2015 / Revised Mar. 23, 2016
Project supported by the National Natural Science Foundation of China (Nos. 11272198 and 11572183)
† Corresponding author, E-mail: dongyh@staff.shu.edu.cn

particle-laden flow is considerably significant to understand the mechanisms of heat transfer between two phases.

In past decades, many experimental and numerical studies of heat transfer in the particle-free turbulent flow have been performed[5–9]. Many thermal quantities, including the mean temperature, turbulent heat fluxes and diffusive sublayer thickness, etc., have been examined, and some mechanisms of heat transfer in the turbulent flow have been understood. It was found that the turbulent heat transfer is mainly characterized by the Prandtl number of the fluids besides the Reynolds number[10]. Redjem-Saad et al.[11] investigated the effect of low to intermediate Prandtl number on the turbulent heat transfer in pipe flows under the isoflux wall condition. They found that the temperature streamwise spectra increase significantly with increasing the Prandtl number at intermediate and high wave numbers, suggesting that the small scales are gradually damped by the enhanced conductive effect with the decrease of the Prandtl number. Recently, the effects of the particles on the heat transfer in the turbulent flow were investigated. Zonta et al.[12] studied the influence of dispersed micrometer size particles on turbulent heat transfer mechanisms in the channel flow and showed that, with respect to the single-phase flow, heat transfer fluxes at the walls increase by roughly 2% when the flow is particle-laden with the smaller particles and an opposite trend for the flow with larger particles. A study by Kuerten et al.[13] found the ratio of particles and fluid specific heat plays a significant impact on the heat transfer, by means of direct numerical simulation (DNS) of gas-particle turbulent flow in the vertical channel with high specific heat capacity particles. Jaszczur[14–15] analyzed the heat transfer and thermal interaction between the particles and fluid in the non-isothermal fully-developed suspension channel flow. However, to date, most works mainly focus on the modulation of different properties of the particles on the heat transfer of turbulent flow, and the effect of the particles on the heat transfer in the turbulent flow with different fluid thermal properties (such as Prandtl number) is rarely considered. Since the particles have different effects on the thermal field of turbulence with different fluid thermal parameters, the study of heat transfer between the particles and turbulence with different thermal properties is absolutely essential in both applications and fundamentals.

The literature survey reveals that there is no DNS of turbulent heat transfer in the particle-laden turbulent channel flow at different Prandtl numbers. In this paper, we firstly present the DNS which investigates the modulation of the particles on the turbulent thermal statistics in the particle-laden flow for different Prandtl numbers. The present paper is structured as follows: the governing equations and the numerical method are described in Section 2. The results of the turbulent thermal statistics (mean temperature, the root mean square (RMS) of temperature fluctuations, turbulent heat flux, the correlation coefficient, and the thermal streaky structure) are discussed in Section 3. Section 4 is the conclusion of this work.

2 Governing equations and numerical methodology

In this section, we perform a DNS of non-isothermal turbulent channel flow with the particles. 200 000 particles are injected into the flow at the random position throughout the channel. Represent the motion of a particle with the density $\rho_{\mathrm{p}} = 2\ 400\ \mathrm{kg/m^3}$ much greater than that of the surrounding carrier phase fluid, and a diameter of a particle ($d_{\mathrm{p}} = 140\ \mu\mathrm{m}$) smaller than the smallest scales of turbulence (Kolmogrov scale). A simple force balance yields equations for the particle position ($x_{\mathrm{p},i}$), the velocity ($v_i = \mathrm{d}x_{\mathrm{p},i}/\mathrm{d}t$) and the temperature ($T_{\mathrm{p}}$):

$$\frac{\mathrm{d}v_i}{\mathrm{d}t} = \frac{\overline{u}_i - v_i}{\tau_{\mathrm{p}}}(1 + 0.15Re_{\mathrm{p}}^{0.687}), \quad \frac{\mathrm{d}T_{\mathrm{p}}}{\mathrm{d}t} = \frac{T_{\mathrm{f}} - T_{\mathrm{p}}}{\tau_{\mathrm{T}}}(1 + 0.3Re_{\mathrm{p}}^{\frac{1}{2}}Pr^{\frac{1}{3}}), \tag{1}$$

where $\overline{u}_i$ and T_{f} is the fluid velocity and temperature at the particle position, respectively. $Re_{\mathrm{p}} = d_{\mathrm{p}}\left|v_i - \overline{u}_i\right|/\nu$ is the particle Reynolds number. While $\tau_{\mathrm{p}} = \rho_{\mathrm{p}}d_{\mathrm{p}}^2/(18\mu)$ and $\tau_{\mathrm{T}} =$

$C_{\mathrm{p,p}}\rho_{\mathrm{p}}d_{\mathrm{p}}^2/(12k_{\mathrm{f}})$ are, respectively, the particle velocity relaxation time and the particle temperature relaxation time. Here, ρ_{p}, d_{p}, and $C_{\mathrm{p,p}}$ are the particle density, the diameter, and the particle specific heat capacity, respectively. The motion equations of the particles are advanced in time by a second-order Adams-Bashforth method. The fourth-order Lagrangian polynomial is used to interpolate the fluid velocity and temperature at the particle position. Periodic boundary conditions are used to reintroduce the particle into the computational domain when the particle moves outside the channel in homogeneous directions, whereas the perfectly-elastic collision at the smooth wall is assumed.

Assuming that the fluid is incompressible and Newtonian, the governing equations for the fluid (in dimensionless form) are as follows:

$$\frac{\partial u_i}{\partial t}=-u_j\frac{\partial u_i}{\partial x_j}+\frac{1}{Re_\tau}\frac{\partial^2 u_i}{\partial x_j^2}-\frac{\partial p}{\partial x_i}+\delta_{3,i}+f_{\mathrm{p}}^i,\quad \frac{\partial T}{\partial t}+u_j\frac{\partial T}{\partial x_j}=\frac{1}{Re_\tau Pr}\frac{\partial^2 T}{\partial x_j^2}+q_{\mathrm{p}},\tag{2}$$

where $u_i\,(i=1,2,3)$ represents the velocity components in the spanwise (z), wall-normal (y), and streamwise (x) directions, respectively. p is the kinematic pressure, $\delta_{3,i}$ is the mean streamwise pressure gradient that drives the flow, T is the temperature, the shear Reynolds number is defined as $Re_\tau=u_\tau H/\nu$, based on the shear velocity (u_τ), the half channel height (H), and the fluid kinematic viscosity (ν). The Prandtl number is defined as $Pr=C_{\mathrm{p,f}}\mu/k_{\mathrm{f}}$, based on the fluid specific heat ($C_{\mathrm{p,f}}$), the dynamic viscosity (μ), and the fluid thermal conductivity (k_{f}). f_{p}^i and q_{p} are the momentum-coupling and energy-coupling terms, respectively. The dimensionless formulae of feedback terms are as follows[13]:

$$\begin{aligned}f_{\mathrm{p}}^i&=\frac{1}{VRe_\tau}\sum_{j=1}^{n}3\pi d_{\mathrm{p}}^j(v_i^j-\overline{u}_i^j)(1+0.15Re_{\mathrm{p}}^{0.687}),\\ q_{\mathrm{p}}&=\frac{1}{Re_\tau Pr}\frac{1}{V}\sum_{j=1}^{n}\pi d_{\mathrm{p}}^j(T_{\mathrm{p}}^j-T_{\mathrm{f}}^j)(2+0.6\cdot Re_{\mathrm{p}}^{\frac{1}{2}}\cdot Pr^{\frac{1}{3}}),\end{aligned}\tag{3}$$

where V is the rectangular region, n is the number of particles in each region.

In this study, the DNS calculation is performed in six cases with $Re_\tau=180$. Cases A1, A2, and A3 represent the particle-free flows with $Pr=0.71$, 1.5, and 3.0, respectively. For the particle-laden flow, Cases B1 ($Pr=0.71$), B2 ($Pr=1.5$), and B3 ($Pr=3.0$) consider the influence of particles on the turbulence. The governing equation of fluid is solved using the fractional step method on a staggered grid[16]. Periodic boundary conditions are used in the streamwise and spanwise directions, and no-lip and no-penetration velocity conditions are imposed on the walls. Two different constant temperatures are performed on the bottom and top walls, $T=0.5$ at $y=1$ (the hot wall), $T=-0.5$ at $y=-1$ (the cold wall). The computational domain is $4\pi H\times 2H\times 4\pi H/3$ and is discretized using an Eulerian grid made of 129^3 nodes. The grid spacing is uniform in the streamwise and spanwise directions, and a stretched grid is imposed in the wall-normal direction.

3 Results and discussion

3.1 Validation of results

In order to validate the reliability of our codes, two cases which have the same parameters as those of Refs. [17]–[18] are performed by the DNS, respectively. Our DNS results on 128^3 grid points will be compared with the previous data by Dritselis and Vlachos[17] and Lessani and Nakhaei[18]. In the study of Ref. [17], the DNS of particle-laden turbulent channel flow has been performed on 128^3 grid points. The computational domain is $4\pi H\times 2H\times 2\pi H$ in the streamwise, normal, and spanwise directions. It is identical to the dimension of the domain in the study of Ref. [18]. The Reynolds number based on the channel half -width and the friction

velocity is equal to $Re_\tau = 180$. The dimensionless particle diameter (d_p/H) is 3.866×10^{-3} and the ratio of the particle density to the fluid density ($\rho_\mathrm{d}/\rho_\mathrm{f}$) is 7 333. The total number of the particles is 3.5×10^4. The exchange of momentum between the particles and fluid is taken into account, and the effects of particle collisions have been neglected. The mean velocity profile (u_3) and velocity fluctuation intensity ($u_{i,\mathrm{rms}}$) of the present DNS are compared with the DNS data of Ref. [17]. They are in good agreement with the DNS data in Fig. 1.

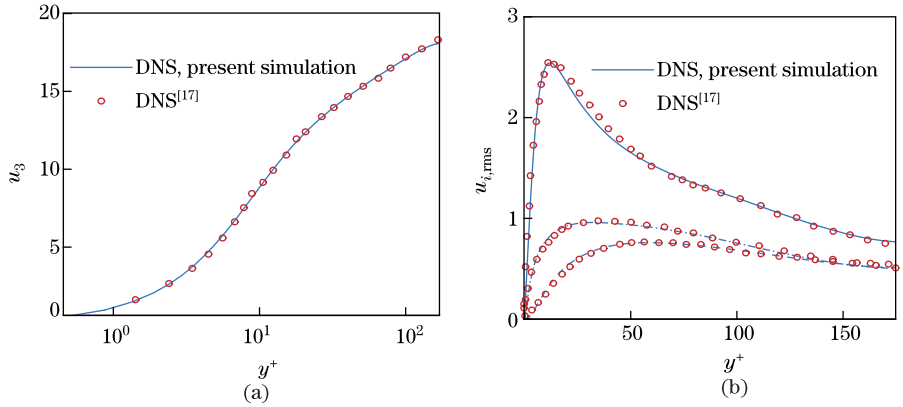

Fig. 1 Turbulent velocity statistics: (a) mean streamwise velocity (u_3); (b) velocity fluctuation ($u_{i,\mathrm{rms}}$) compared with DNS data of Ref. [17]

Lessani and Nakhaei[18] performed the large eddy simulation (LES) with the dynamic model on 64^3 grid points for the particle-laden channel flow with the thermal field. The Prandtl number and Reynolds number are 0.7 and 180, respectively. The heat transfer between two phases is considered. The particle diameter and density are the same with those of Ref. [17], and the total number of the particles is 10^5. In addition, the ratio of particle specific heat capacity to the fluid specific heat ($C_{\mathrm{p,p}}/C_{\mathrm{p,f}}$) is 1.8. The mean temperature profiles of fluid and the particle along the normal direction are shown in Fig. 2. By comparison, our results are accurate and reliable.

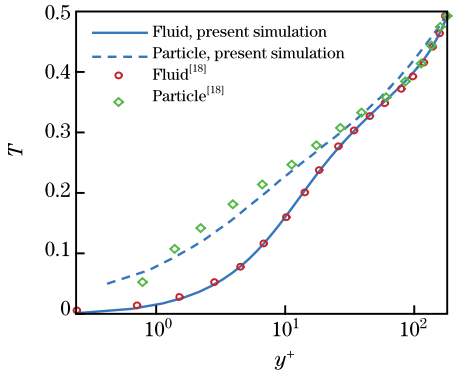

Fig. 2 Mean temperatures of fluid and particle compared with LES data of Ref. [18]

3.2 Mean temperature

The dimensionless mean temperature distribution normalized by the friction temperature ($T_\tau = q_\mathrm{w}/(\rho_\mathrm{f} C_{\mathrm{p,f}} u_\tau)$, and q_w is the wall heat flux) is shown in Fig. 3(a) as a function of the wall distance for three Prandtl numbers ($Pr = 0.71$, 1.5, 3.0) at $Re_\tau = 180$. Similar to the

mean velocity distribution, there also exists the logarithmic region in the mean temperature ($T^+ = c_\mathrm{T} + \ln(y^+)/k_\mathrm{T}$), where k_T is the von Karman constant of the mean temperature. In the present simulation, the predicted profile in the logarithmic region for the particle-free flow is in good agreement with Kader's correlation[6]. The conductive sublayer thickness becomes gradually thinner when the Prandtl number increases and that is consistent with the results of Ref.[8]. With the existence of the particles, the conductive sublayer thickness is decreased for all Prandtl numbers, and the normalized mean temperature T^+ of particle-laden flow is smaller than that of particle-free flow in Fig. 3(a).

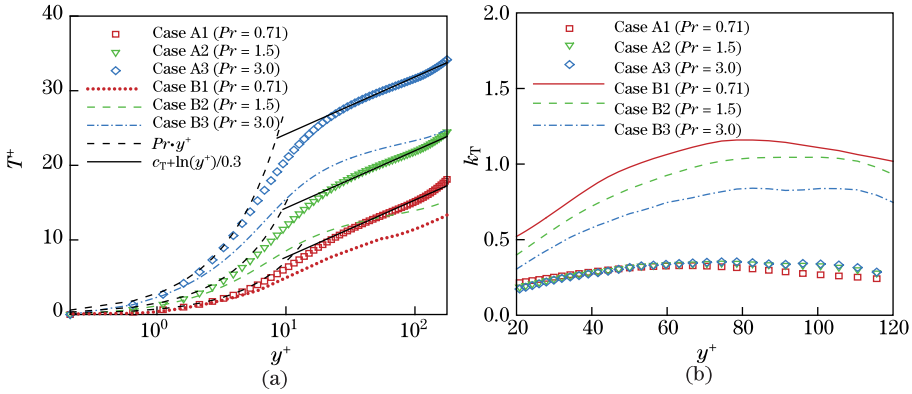

Fig. 3 (a) Normalized mean temperature of fluid; (b) distribution of von Karman constant (k_T) for three Prandtl numbers

Due to the use of the present DNS data, an accurate determination of k_T can be obtained by the relationship ($k_\mathrm{T} = (\mathrm{d}T^+/\mathrm{d}y^+)^{-1}/y^+$), and Fig. 3(b) shows the distribution of k_T for three Prandtl numbers. Obviously, k_T is independent of Prandtl number and is almost constant ($k_\mathrm{T} \approx 0.3$) in the logarithmic region for particle-free flows, which agrees with the study of Ref. [7]. However, the particles have significant influence on the von Karman constant for different Prandtl numbers. For the particle-laden flow with three Prandtl numbers, the von Karman constant increases due to the addition of particles, and the increase of k_T is more obvious for the smaller Prandtl number.

3.3 RMS of temperature fluctuations and turbulent heat fluxes

The RMS of temperature fluctuations (T^+_rms) normalized by the friction temperature is shown in Fig. 4. With the increase of Prandtl number, the temperature fluctuation intensity becomes stronger, and the peak of the temperature intensity becomes larger and closer to the wall. That agrees with the study of Ref. [11]. However, the intensity of temperature fluctuations is significantly decreased for three Prandtl numbers by the particles. Turbulent heat fluxes normalized by the friction velocity and temperature for three Prandtl numbers are shown in Fig. 5. Obviously, with the presence of the particles, the wall-normal turbulent heat flux ($u_2'^+T'^+$) and streamwise turbulent heat flux ($u_3'^+T'^+$) are also reduced. The location of the peak value of the streamwise turbulent heat flux shifts towards the channel center for the particle-laden flow.

In order to investigate the extent of the influence of the particles on turbulent thermal statistics, the change rate of thermal statistics can be defined as follows:

$$\Theta_\theta = \frac{\theta_\text{particle-laden} - \theta_\text{particle-free}}{\theta_\text{particle-free}}, \tag{4}$$

where $\theta_\text{particle-laden}$ and $\theta_\text{particle-free}$ represent thermal statistics of particle-laden and particle-free flow, respectively. The change rates of temperature fluctuation intensity $\Theta_{T'}$ and turbulent heat fluxes $\Theta_{u_i'T'}$ are shown in Fig. 6. Apparently, the change rates of temperature fluctuation

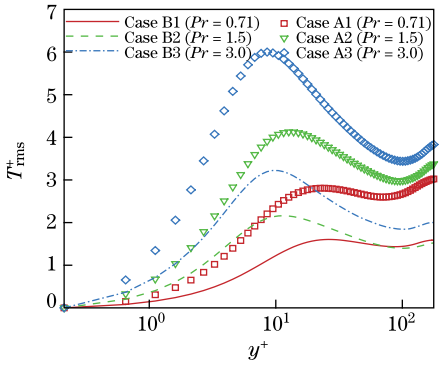

Fig. 4 Normalized RMS of temperature fluctuations $T^+_{\rm rms}$

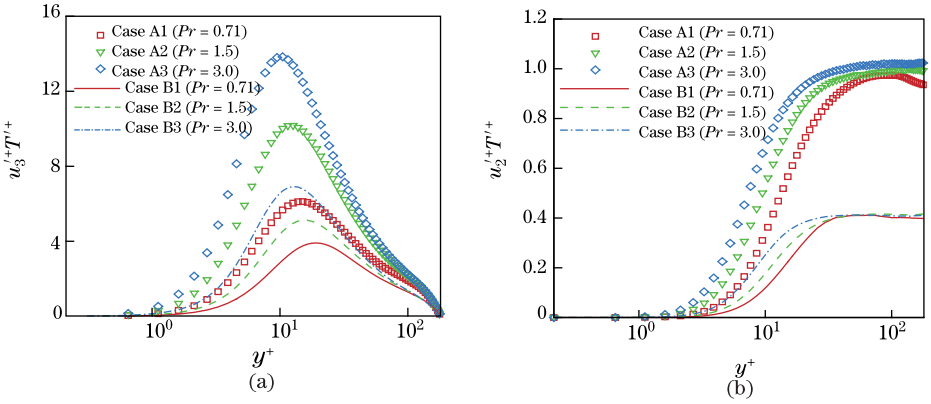

Fig. 5 Turbulent heat fluxes: (a) streamwise direction; (b) wall-normal direction

intensity and turbulent heat fluxes are monotonically decreasing with the increase of Prandtl number. That indicates that the particles have more significant influence on the thermal field of turbulence with the smaller Prandtl number. Additionally, the peak position of the change rate of turbulent heat fluxes mainly occurs near the wall, as shown in Fig. 6(b), and this possible reason is the cluster of the particles in the near-wall region. In addition, the change rate of the normal-wall turbulent flux ($\Theta_{u_2'T'}$) is always larger than that of the streamwise turbulent flux ($\Theta_{u_3'T'}$) for three Prandtl numbers. The reason for this is that the particles have more effects on normal-wall velocity fluctuations than streamwise velocity fluctuations.

3.4 Nusselt number

In order to measure the influence of the particles on the heat transfer in the turbulent flow with different Prandtl numbers, we define the Nusselt number as follows (in the dimensionless form):

$$Nu = \frac{2H}{T_h - T_c}\frac{\mathrm{d}\langle T\rangle}{\mathrm{d}y}\bigg|_{y=-1}. \tag{5}$$

For the particle-laden turbulent flow, the Nusselt number (Nu) can be decomposed into three parts[13]:

$$Nu = \underbrace{1}_{Nu_{\rm v}} + \underbrace{Re_\tau Pr\int_{-1}^{1}\langle T'u_2'\rangle\,\mathrm{d}y}_{Nu_{\rm T}} + \underbrace{Re_\tau Pr\int_{-1}^{1}(1-y)\langle q_{\rm p}\rangle\mathrm{d}y}_{Nu_{\rm feed}}, \tag{6}$$

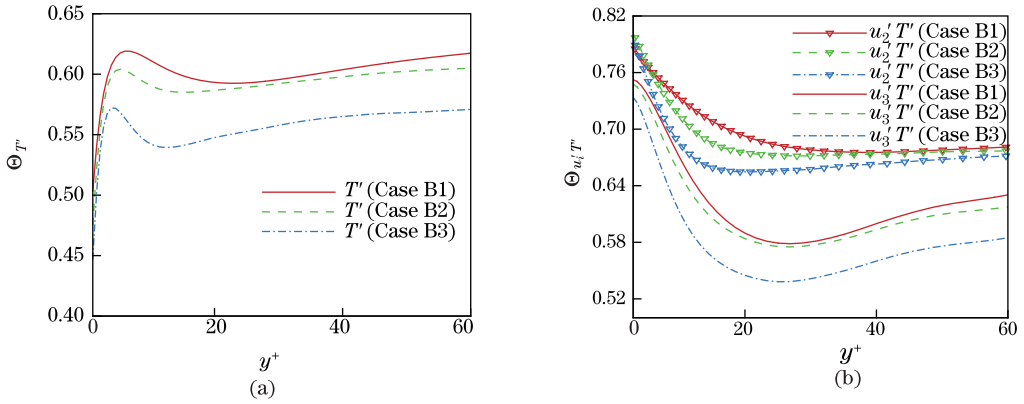

Fig. 6 Change rate of thermal statistics: (a) temperature fluctuations ($\Theta_{T'}$); (b) turbulent heat flux ($\Theta_{u_i'T'}$)

where Nu_{v}, Nu_{T}, and Nu_{feed} represent the contribution of a constant viscous, turbulent convection, and the particle thermal feedback to heat transfer, respectively.

Table 1 shows the three different contributions to the heat transfer of turbulent flow with different Prandtl numbers in this paper. For the particle-free flow (Cases A1, A2, and A3), when the Prandtl number increases, the total Nusselt number (Nu) and the turbulent Nusslet number (Nu_{T}) gradually increase, which can be found from Refs. [19]–[20]. For the particle-laden flow with three different Prandtl numbers, the particles reduce the total Nusselt number (Nu) and the turbulent Nusslet number (Nu_{T}). Moreover, it is found that the particle feedback Nusselt number (Nu_{feed}) increases as the Prandtl number increases.

Additionally, to measure the extent of the influence of the particles to heat transfer for the turbulent channel flow with three Prandtl numbers, two parameters can be defined, namely, the change rate (ϕ) of the turbulent Nusselt number and the ratio (η) of Nusselt number of the particles feedback to the total Nusselt number, i.e.,

$$\phi = \left| \frac{Nu_{\mathrm{T,particle\text{-}laden}} - Nu_{\mathrm{T,particle\text{-}free}}}{Nu_{\mathrm{T,particle\text{-}free}}} \right| \times 100\%, \quad \eta = \frac{Nu_{\mathrm{feed}}}{Nu} \times 100\%, \tag{7}$$

where $Nu_{\mathrm{T,particle\text{-}laden}}$ and $Nu_{\mathrm{T,particle\text{-}free}}$ represent the turbulent Nusselt number of particle-laden and particle-free flows, respectively. From Table 1, it can be found that the change rate (ϕ) of turbulent Nusselt number is larger for the particle-laden flow with the smaller Prandtl number. That illustrates that the suppression of convective heat transfer of turbulence induced by particles becomes more evident for the smaller Prandtl number. It is consistent with the change rate of normal-wall turbulent heat flux. In addition, it is clarified that the ratio (η) of the feedback Nusselt number to the total Nusselt number gradually decreases with the increase of Prandtl numbers. That indicates that the contribution to heat transfer from thermal feedback of the particles becomes smaller for the larger Prandtl number. As described above, the thermal field of turbulence with the smaller Prandtl number can be easily affected by particles.

Table 1 Different contributions to Nusselt number for different Prandtl numbers

Case	A1	A2	A3	B1	B2	B2
Pr	0.71	1.5	3.0	0.71	1.5	3.0
Nu	7.10	11.5	15.9	6.90	10.1	13.7
Nu_{T}	6.10	10.5	14.9	3.10	5.8	8.4
Nu_{feed}	—	—	—	2.80	3.3	4.3
η/%	—	—	—	40.60	32.7	31.4
ϕ/%	—	—	—	49.20	44.7	43.6

3.5 Correlation coefficients

The turbulent thermal field is associated with the turbulent velocity field. For the particle-laden flow, the turbulent velocity field is modulated by the particles that results the modulation of turbulent velocity field has influence on the turbulent thermal filed. In order to investigate the interconnection between turbulent velocity field and the thermal field in the particle-laden flow, correlation coefficients between velocity fluctuations and temperature fluctuations ($R_{u_iT} = \langle u_i' T' \rangle / (u_{i,\mathrm{rms}} T_{\mathrm{rms}})$) for different Prandtl numbers[21] are shown in Fig. 7. The correlation coefficients R_{u_2T} and R_{u_3T} gradually decease with the increase of Prandtl number. That indicates that the interconnection between the turbulent velocity and thermal field becomes gradually weak as the Prandtl number increases. Therefore, it is illustrated that the modulation of turbulent velocity field induced by the particles has more significant impact on the turbulent thermal field for the particle-laden flow with the smaller Prandtl number.

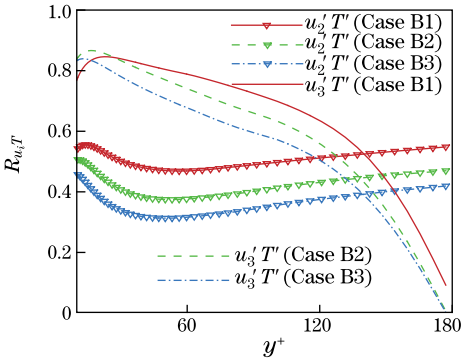

Fig. 7 Correlation coefficient between velocity fluctuations and temperature fluctuations (R_{u_iT})

In addition, the turbulent thermal field is directly connected with the temperature of the particles besides the turbulent velocity field. The heat exchange between turbulence and particles is analyzed in Fig. 8. Obviously, the heat exchange between two phases becomes more depressive for the particle-laden flow with the larger Prandtl number, and thermal feedback of the particles on turbulence (q_{p}) becomes weaker. The correlation coefficient of the particles and turbulence temperature fluctuations is further investigated. The correlation coefficient of the particles and turbulence temperature fluctuations is defined as follows:

$$R_{TT_{\mathrm{p}}} = \frac{\langle T' T_{\mathrm{p}}' \rangle}{T_{\mathrm{rms}} T_{\mathrm{p,rms}}}, \tag{8}$$

where T_{p}' and T' are the particle and fluid temperature fluctuations at the particle position, respectively. And $T_{\mathrm{p,rms}}$ and T_{rms} are RMSs of the particle and fluid temperature fluctuations at the particle position. Figure 9 shows the correlation coefficient of the particles and fluid temperature fluctuations ($R_{TT_{\mathrm{p}}}$) becomes smaller with the increase of Prandtl number. That further explains that the influence of the particles on the turbulent thermal field with the larger Prandtl number becomes weaker.

3.6 Structure of temperature fluctuations

To explore the effects of the particles on the thermal structures for various Prandtl numbers, instantaneous temperature fluctuations in the near-wall region are visualized in Fig. 10. For the particle-free flow, it is obvious that thermal streaks become more pronounced with the increase of Prandtl number in Figs. 10(a) and 10(c). That is consistent with the study of Ref. [11]. Due to the existence of the particles, the thermal streaks become more continuous and more persistent in the near-wall region in Figs. 10(b) and 10(d). Furthermore, the particles have

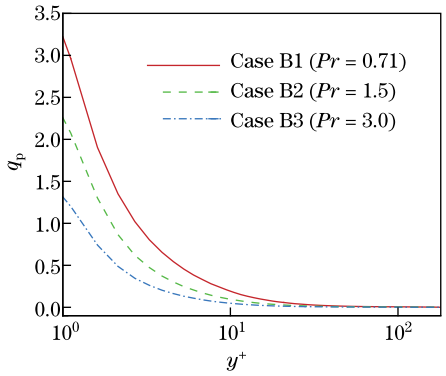

Fig. 8 Thermal feedback of particles on turbulence (q_p)

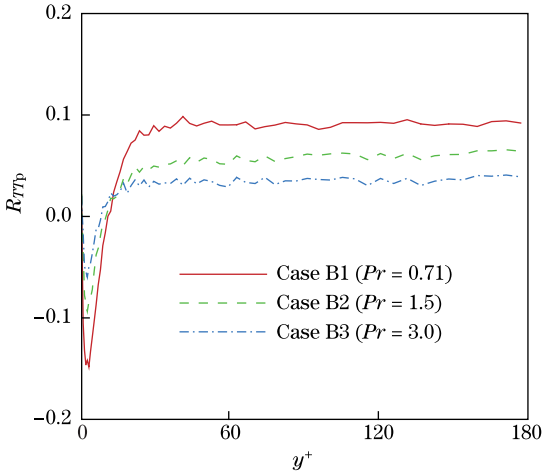

Fig. 9 Correlation coefficient of particle temperature fluctuation and fluid temperature fluctuation (R_{TT_p})

more significant influence on the thermal streaks for $Pr = 0.71$. Because of the correlation between the thermal and the velocity field, the thermal streaks are affected by the succession of bursting motion. For the larger Prandtl number, the relevance between thermal and velocity field reduces, which causes ejection and sweep events to have less influence on the thermal streaks.

Higher-order statistics such as skewness ($S(T') = \langle T'^3 \rangle / T'^3_{\mathrm{rms}}$) are analyzed. A high positive value of the skewness means that the temperature fluctuations obtain large positive rather than negative values more frequently. Obviously, the particles reduce the value of $S(T')$, and the tendency is more evident for the smaller Prandtl number near the wall, as shown in Fig. 11. It implies that the frequency of the temperature fluctuations characterized by low-temperature streaks becomes larger. That is consistent with the modulation of the thermal streaky structures induced by the particles for different Prandtl numbers.

4 Conclusions

In the present work, the influence of the particles on the turbulent thermal field with three Prandtl numbers ($Pr = 0.71$, 1.5, and 3.0) is investigated by the DNS combined with the

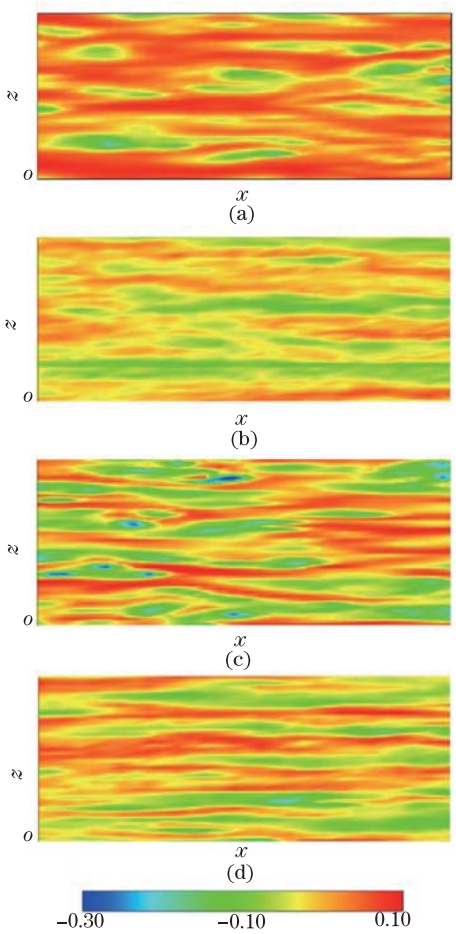

Fig. 10 Instantaneous temperature fluctuation contours of wall-parallel plane located at $y^+ = 3.5$, (a) $Pr = 0.71$, particle-free flow; (b) $Pr = 0.71$, particle-laden flow; (c) $Pr = 3.0$, particle-free flow; (d) $Pr = 3.0$, particle-laden flow

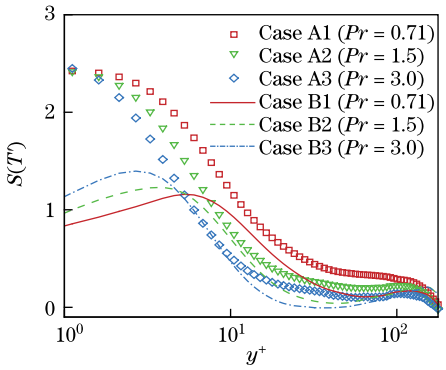

Fig. 11 Skewness of temperature fluctuation ($S(T')$)

Lagrangian particle tracking method. Compared with results of particle-free flow, the particles reduce the normalized mean temperature, temperature fluctuations, and turbulent heat fluxes

for the particle-laden flow with three Prandtl numbers. Furthermore, the convective heat transfer of turbulence is suppressed by particles. In addition, some parameters are defined, such as the change rate of thermal statistics, the ratio of the particles feedback Nusselt numbers to the total Nusselt numbers (η), and the change rate of the turbulent Nusselt number (ϕ), to investigate the extent of the influence of the particles on the turbulent thermal field. It is shown that the weakening of temperature fluctuations and turbulent heat fluxes induced by particles is more evident for the particle-laden flow with the smaller Prandtl number.

By investigating the interconnection between the turbulent thermal field and the turbulent velocity field, it is found that the modulation of velocity field induced by the particles has less influence on the turbulent thermal field of the particle-laden flow with the larger Prandtl number. In addition, the heat exchange between the turbulence and the particles gradually decreases as the Prandtl number increases. The reasons explain that the modulation of the particles on the turbulent thermal field with the small Prandtl number is more obvious than that for the large Prandtl number.

References

[1] Barigou, M., Mankad, S., Fryer, P. J. Heat transfer in two-phase solid-liquid food flows: a review. *Food and Bioproducts Processing*, **76**, 3–29 (1998)

[2] Rashidi, M. M., Hosseini, A., Pop, I., Kumar, S., and Freidoonimehr, N. Comparative numerical study of single and two-phase models of nanofluid heat transfer in wavy channel. *Applied Mathematics and Mechanics* (*English Edition*), **35**, 831–848 (2014) DOI 10.1007/s10483-014-1839-9

[3] Salari, M., Mohammadtabar, M., and Mohammadtabar, A. Numerical solutions to heat transfer of nanofluid flow over stretching sheet subjected to variations of nanoparticle volume fraction and wall temperature. *Applied Mathematics and Mechanics* (*English Edition*), **35**, 63–72 (2014) DOI 10.1007/s10483-014-1772-8

[4] Anbuchezhian, N., Srinivasan, K., Chandrasekaran, K., and Kandasamy, R. Thermophoresis and Brownian motion effects on boundary layer flow of nanofluid in presence of thermal strantification due to solar energy. *Applied Mathematics and Mechanics* (*English Edition*), **33**, 765–780 (2012) DOI 10.1007/s10483-012-1585-8

[5] Kim, J. and Moin, P. Transport of passive scalars in a turbulent channel flow. *Turbulent Shear Flows*, **6**, 85–96 (1989)

[6] Kasagi, N., Tomita, Y., and Kuroda, A. Direct numerical simulation of passive scalar field in a turbulent channel flow. *Journal of Heat Transfer*, **114**, 598–606 (1992)

[7] Kasagi, N. and Ohtsubo, Y. Direct numerical simulation of low Prandtl number thermal field in a turbulent channel flow. *Turbulent Shear Flows*, **8**, 97–119 (1993)

[8] Kawamura, H., Abe, H., and Matsuo, Y. DNS of turbulent heat transfer in channel flow with respect to Reynolds and Prandtl number effects. *International Journal of Heat and Fluid Flow*, **20**, 196–207 (1999)

[9] Kawamura, H., Abe, H., and Shingai, K. DNS of turbulence and heat transport in a channel flow with different Reynolds and Prandtl numbers and boundary conditions. *Proceedings of the* 3*rd International Symposium on Turbulence, Heat and Mass Transfer*, Aichi Shuppan Press, Japan, 15–32 (2000)

[10] Na, Y., Papavassiliou, D. V., and Hanratty, T. J. Use of direct numerical simulation to study the effect of Prandtl number on temperature fields. *International Journal of Heat and Fluid Flow*, **20**, 187–195 (1999)

[11] Redjem-Saad, L., Ould-Rouiss, M., and Lauriat, G. Direct numerical simulation of turbulent heat transfer in pipe flows: effect of Prandtl number. *International Journal of Heat and Fluid Flow*, **28**, 847–861 (2007)

[12] Zonta, F., Marchioli, C., and Soldati, A. Direct numerical simulation of turbulent heat transfer modulation in micro-dispersed channel flow. *Acta Mechanica*, **195**, 305–326 (2008)

[13] Kuerten, J. G. M., van der Geld, C. W. M., and Geurts, B. J. Turbulence modification and heat transfer enhancement by inertial particles in turbulent channel flow. *Physics of Fluids*, **23**, 123301–123309 (2011)

[14] Jaszczur, M. Numerical analysis of a fully developed non-isothermal particle-laden turbulent channel flow. *Archives of Mechanics*, **63**, 77–91 (2011)

[15] Jaszczur, M. A numerical simulation of the passive heat transfer in a particle-laden turbulent flow. *Direct and Large-Eddy Simulation* VIII (eds. Kuerten, H., Geurts, B., Armenio, V., and Fröhlich, J.), Springer-Verlag, Berlin, 195–200 (2011)

[16] Dong, Y. H. and Chen, L. F. The effect of stable stratification and thermophoresis on fine particle deposition in a bounded turbulent flow. *International Journal of Heat and Mass Transfer*, **54**, 1168–1178 (2011)

[17] Dritselis, C. D. and Vlachos, N. S. Large eddy simulation of gas-particle turbulentchannel flow with momentum exchange between the phases. *International Journal of Multiphase Flow*, **37**, 706–721 (2011)

[18] Lessani, B. and Nakhaei, M. H. Large-eddy simulation of particle-laden turbulent flow with heat-transfer. *International Journal of Heat and Mass Transfer*, **67**, 974–983 (2013)

[19] Kawamura, H., Ohsaka, K., Abe, H., and Yamamoto, K. DNS of turbulent heat transfer in channel flow with low to medium-high Prandtl number fluid. *International Journal of Heat and Fluid Flow*, **19**, 482–491 (1998)

[20] Ould-Rouiss, M., Redjem-Saad, L., Lauriat, G., and Mazouz, A. Effect of Prandtl number on the turbulent thermal field in annular pipe flow. *International Communications in Heat and Mass Transfer*, **37**, 958–963 (2010)

[21] Tiselj, I., Pogrebnyak, E., Li, C., Mosyak, A., and Hetsroni, G. Effect of wall boundary condition on scalar transfer in a fully developed turbulent flume. *Physics of Fluids*, **13**, 1028–1039 (2001)